

# GENERATIVE DESIGN AND IEQ PERFORMANCE OPTIMIZATION OF SCHOOL BUILDINGS BASED ON A PARAMETRIC ALGORITHM

## PROJETO GENERATIVO E OTIMIZAÇÃO DE DESEMPENHO IEQ DE EDIFÍCIOS ESCOLARES COM BASE EM UM ALGORITMO PARAMÉTRICO

Sahar Mohammadi<sup>1</sup>  
Yousef Gorji Mahlabani<sup>2</sup>  
Fariborz Karimi<sup>3</sup>  
Babak MohammadHoseini<sup>4</sup>

### Abstract

This research aims to examine the potential of generative and optimization algorithms in the early stage of a school building design in Tabriz to achieve better IEQ. It also investigates the compatibility of the evolutionary optimization tools combined with a parametric model in stimulating building comfort performance in achieving an optimized design. This process includes four steps: defining the parametric building model, defining its material and construction properties, stimulation of thermal and visual comfort and carbon dioxide concentration, optimization, and choosing the best result. The adaptive PMV model is used for thermal comfort, imageless daylight glare probability is used for visual comfort, and a CO<sub>2</sub> concentration is used for IAQ assessment. It was found that the performance of the options introduced by the algorithm is more appropriate than the design prototype. However, the results show that the samples are acceptable in carbon dioxide concentration. What needs further investigation is thermal and visual comfort. Among the studied variables on IEQ performance, the WWR ratio of the southern wall had the most significant impact. Based on the optimization results, thermal comfort changed in the range of 10%, visual comfort in the range of 30%, and CO<sub>2</sub> concentration in the range of 0.19%.

**Keywords:** Indoor environment quality, Generator design algorithm, Optimization algorithm, Genetic algorithm, Thermal comfort.

### Resumo

Esta pesquisa tem como objetivo examinar os potenciais de algoritmos generativos e de otimização na fase inicial de um projeto de edifício escolar em Tabriz para obter um melhor IEQ. Também investiga a compatibilidade das ferramentas de otimização evolutiva combinadas com um modelo paramétrico para estimular o desempenho de conforto de construção na obtenção de um design otimizado. Este processo inclui quatro etapas: definição do modelo paramétrico de construção, definição de suas propriedades materiais e construtivas, estimulação do conforto térmico e visual e da concentração de dióxido de carbono, otimização e escolha do melhor resultado. O modelo adaptativo PMV é usado para conforto térmico, a probabilidade de ofuscamento da luz do dia sem imagens é usada para conforto visual, uma concentração de CO<sub>2</sub> é usada para avaliação de IAQ. A investigação revelou que o desempenho das opções introduzidas pelo algoritmo é mais adequado do que o protótipo de projecto. No entanto, os resultados mostram que as amostras são aceitáveis na concentração de dióxido de carbono. É necessário mais investigação para conforto térmico e visual. Dentre as variáveis estudadas sobre o desempenho do IEQ, a relação WWR da parede sul teve o impacto mais significativo. Com base nos resultados da otimização, o conforto térmico mudou na faixa de 10%, o conforto visual na faixa de 30% e a concentração de CO<sub>2</sub> na faixa de 0,19%.

**Palavras-chave:** Qualidade do ambiente interno, Algoritmo de projeto generativo, Algoritmo de otimização, Algoritmo genético, Conforto térmico.

<sup>1</sup> Imam Khomeini International University, <https://orcid.org/0000-0002-8848-2782>, sahar.mo@gmail.com

<sup>2</sup> Imam Khomeini International University, <https://orcid.org/0000-0003-3711-8494>, gorji@arc.ikiu.ac.ir

<sup>3</sup> Imam Khomeini International University, <https://orcid.org/0000-0003-3592-9162>, f.karimi@arc.ikiu.ac.ir

<sup>4</sup> Imam Khomeini International University, <https://orcid.org/0000-0002-4102-4047>, b\_m\_hosseini@sci.ikiu.ac.ir

## INTRODUCTION

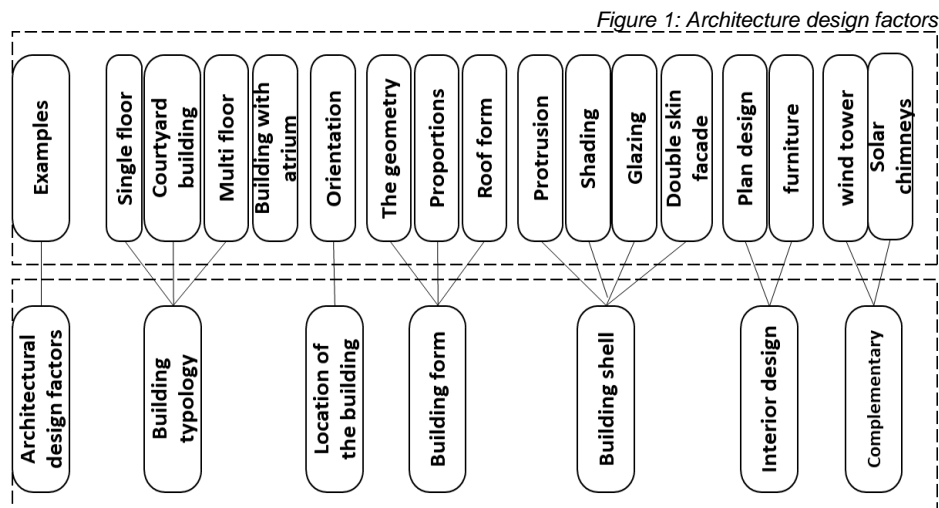
Interior environment quality (IEQ) is a factor that, according to recent research projects, has a direct relationship with the health and efficiency of the occupant in office and educational environments [1-3]. Thermal, visual, and acoustic comfort, as well as indoor air quality, are components that influence it [4, 5]. To provide each of the above components within a range of human comfort, energy consumption is required to provide cooling, heating, lighting, and ventilation [6, 7]. Therefore, the two indicators of building energy consumption and indoor quality are related. Creating conditions to reduce energy consumption in a building requires a strategic approach to developing the principles and processes of architectural design.

Among the variety of constructions, schools, where children spend most of their time, are one of the important ones whose design influences the quality of learning [8].

IEQ can be assessed through objective physical measurements and subjective occupant surveys in existing buildings and surveys of design criteria used for energy calculation or annual energy performance simulation (for existing or under-construction buildings) [9, 10].

Architectural design factors significantly affect the provision of comfort in a building. Numerous studies have been conducted on the relationship between form parameters on a single building scale [11]. Design factors are based on the architectural design process and are divided into six categories: building typology, orientation, building form, building shell, interior design, and complementary components. The subsets of each group are shown in figure 1.

The indoor conditions are influenced by numerous elements, like the design factors defined in figure 1. For instance, one of the crucial options affected is the glazing ratio, due to its potential to reduce or increase indoor comfort conditions (visual, acoustic, and thermal) [12]. However, knowing its perfect amount before a design is more beneficial than assessing its efficiency after building construction.



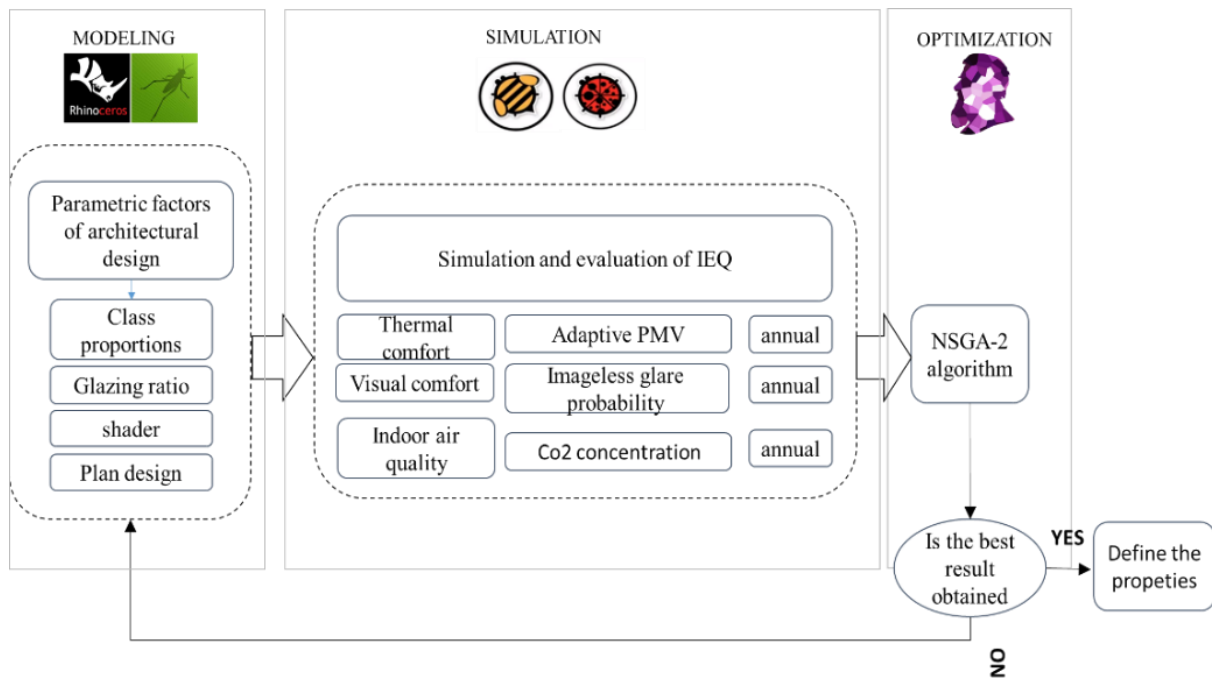
Parametric models and optimization tools are efficient ways to achieve the desired goals in decision-making problems [13, 14]. Parametric modeling is used for both simulation and optimization purposes. Optimization models are based on mathematical algorithms that can determine the best and most optimal solutions to problems, and these solutions are mostly accurate and increase the benefits [15]. Genetic algorithms are a computational technique based on the disciplines of evolution that were initially introduced in the 1960s by John Holland and were developed in the 1970s [16]. John Fraser is widely regarded as the founder of the evolutionary digital design process and a pioneer of productive design, in which he employed algorithms to solve architectural issues [17]. These algorithms emerged in architecture mostly to study the complex problems in building performance and architectural form findings [18, 19]. This article defines the school building as a parametric model and then optimizes it using the simulation and optimization tools in the Grasshopper plug-in to use the simulation method of the IEQ assessment in the early design stage.

## METHODOLOGY

The workflow of this paper consists of an automated process of modeling, simulation, and optimization evaluation, which is written on Grasshopper software. Many plugins and simulation engines are involved in this process, as follows: Grasshopper will be responsible for parametric modeling in the first part. In the second part, Ladybug and Honeybee will simulate building performance in terms of thermal comfort and CO<sub>2</sub> concentrations using Energy-Plus and Open Studio engines. They also use the Radiance engine for glare analysis. In the last part, the genetic algorithm is prepared to optimize the solutions through the Wallacei plugin, which can perform multi-objective optimization through the NSGA-2 algorithm. The combinations of parameters such as class dimension, glazing percentage, and shading devices lead to different performances in IEQ [20]. There are numerous indicators from which to evaluate performance; thus, the best indicator is used for each parameter, as illustrated in figure 2.

The framework begins with creating a generative algorithm that creates different floor plans according to defined parameters. The process continues with converting the plan to zones, defining their glazing areas and shading devices, and then setting their materials. Then, the thermal and visual comfort and IAQ simulation settings were performed. Wallacei creates different school models by modifying defined number sliders and gene pools. Then, it performs optimization by simulating and evaluating the values of three defined functions. The workflow's setup is discussed step-by-step. The process is divided into three phases: generation, which includes creating masses; installing windows; adding shading devices and setting materials; simulation, which contains thermal and visual comfort and Co<sub>2</sub> concentration simulation; optimization (Figure 2).

Figure 2: the workflow



## Generative Design and Modification

To design the parametric model of the school, 71 samples of schools in Tabriz were examined. The results showed that in the plans, the corridor was considered the central space, and the classrooms and other spaces were organized around it. Figure 3 shows some examples of school buildings. Studies on thermal comfort have proven the effects of building orientation [21, 22], type of materials [23], amount of glazing [24, 25], space dimensions, type of shade [26], and size. In the case of visual comfort, the size of windows and shades is also acceptable [27, 28]. To conduct this research, the following variables have been considered, and the rest of the factors are considered constant.

- 1- Dimensions of classrooms with the fixed area, 2-Percentage of window area on a wall, 3-Shading, 4-Protrusions

The design variables that are set through sliders shape each option of building geometry. The range of each variable was extracted from the samples analyzed. The base case (figure 5) is generated according to the most common plan of Tabriz schools. There are 14 design variables for this model. They are presented in Table 1 and Figure 4.

Figure 3: Sample plans of Tabriz schools: The green color shows the corridor, the grey color shows classes, the blue color represents stairs, the yellow color shows the entrance, and the white color represents office and functional spaces

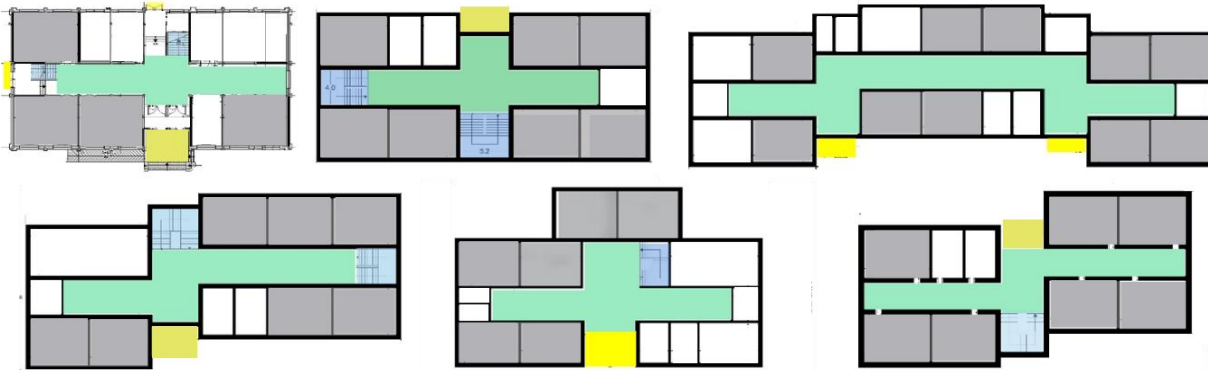
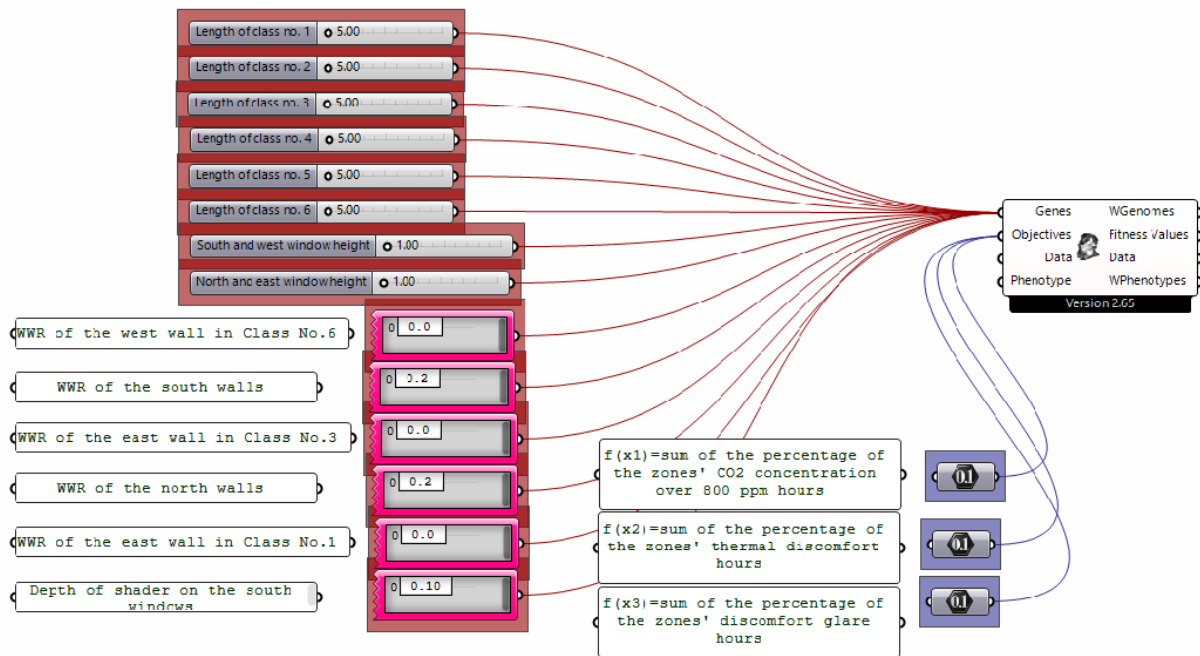


Table 1: variables, ranges, design feature scope, and description.

no	Design variables	Range		Design feature scope	Description
		Min	Max		
V.1	Length of class no. 1	5.00	8.00	Shape	The range is determined based on the reviewed samples of existing schools
v.2	Length of class no. 2	5.00	8.00	Shape	The range is determined based on the reviewed samples of existing schools
v.3	Length of class no. 3	5.00	8.00	Shape	The range is determined based on the reviewed samples of existing schools
v.4	Length of class no. 4	5.00	8.0	Shape	The range is determined based on the reviewed samples of existing schools
v.5	Length of class no. 5	5.00	8.00	Shape	The range is determined based on the reviewed samples of existing schools
v.6	Length of class no. 6	5.00	8.00	Shape	The range is determined based on the reviewed samples of existing schools
v.7	South and west window height	1.0-2.0m		Fenestration	
v.8	North and east window height	1.0-2.0m		Fenestration	
v.9	WWR of the west wall in Class No.6	0-0.9%		Fenestration	0 means a wall without a window, and 0.95 means a glass wall with just a frame.
v.10	WWR of the south walls	0.2-0.9%		Fenestration	Begins with 0.2 cause the wall should have windows. 0.95 means a glass wall with just a frame.
v.11	WWR of the east wall in Class No.3	0-0.9%		Fenestration	0 means a wall without a window, and 0.95 means a glass wall with just a frame.
v.12	WWR of the north walls	0.2-0.9%		Fenestration	Begins with 0.2 cause the wall should have windows. 0.95 means a glass wall with just a frame.
v.13	WWR of the east wall in Class No.1	0-0.9%		Fenestration	0 means a wall without a window, and 0.95 means a glass wall with just a frame.
v.14	Depth of shader on the south windows	0.1-0.9			Only the north windows do not have shaders according to Tabriz's sun path.

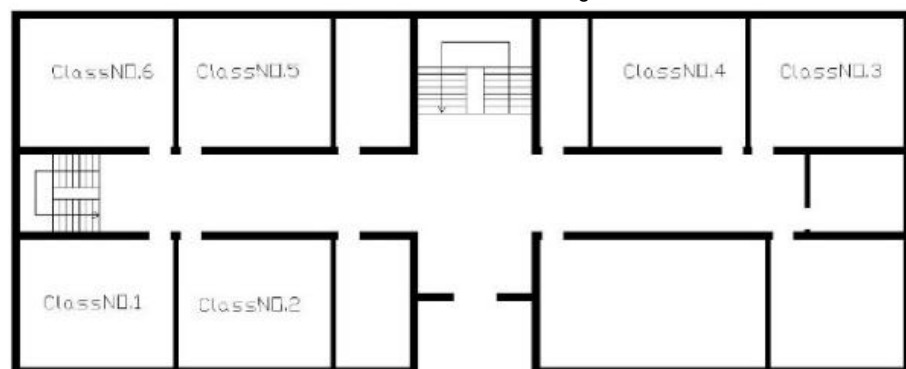
Figure 4. Optimization inputs



The base model of the school is shown in figure 5. It was designed based on the selected sample and includes a corridor in the middle of the plan. In the parametric model, the corridors and stairs, as well as the spaces other than the classrooms, were considered fixed. The classrooms changed in terms of their dimensions and length-to-width ratio. Their position in the plan and their area are considered fixed. The length of each class is chosen between 5 to 8 meters. The width of the class was calculated through the following equation:

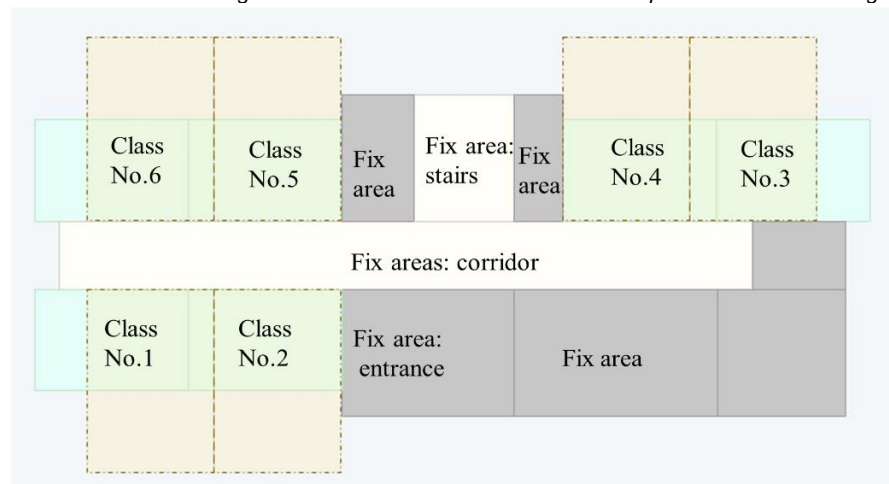
$$\text{Equation (1) } \text{Area} / \text{Class length} = \text{Class width}$$

Figure 5. The base model of research



By considering a fixed area of 42 square meters for classes, the width changes automatically by changing the length. The second floor follows the first floor's plan (figure 6).

Figure 6: How the dimensions of classes in a parametric model change.



After the modeling process, the masses were converted to zones, and the building program was set to secondary school by the Honeybee component. Each building zone's usage was assigned to it. The structural characteristics of the walls, windows, roof, and floor are set according to the Iranian standard construction details, which are presented in Table 2.

Table 2: Construction material assigned to model

<b>Exterior Wall layers details (Inside to outside)</b>				
Layers	Thickness (mm)	Density (kg/m <sup>3</sup> )	Specific Ht. (kJ/[kg - °K])	R-Value ([m <sup>2</sup> - °K]/W)
gypsum plaster	15.00	800	1.09	0.054
Clay block	150.00	1300	0.840	0.39
Wall insulation	50.00	265	0.836	1.04
Clay block	100.0	1300	0.840	0.39
Facade brick	30.00	1700	0.840	0.30
<b>Total U value 0.8482 W/m<sup>2</sup>.K</b>		<b>total R-value: 1.1788 m<sup>2</sup>.K/W</b>		
<b>interior Wall layers details (Inside to outside)</b>				
gypsum plaster	15.00	800	1.09	0.054
Clay block	150.00	1300	0.840	0.39
gypsum plaster	15.00	800	1.09	0.054
<b>Total U value 11.2748 W/m<sup>2</sup>.K</b>		<b>total R-value: 0.08869 m<sup>2</sup>.K/W</b>		
<b>Window material</b>				
Layers	U value (W/m <sup>2</sup> .K)	Solar heat gain coefficient	Visible transmittance	R-Value ([m <sup>2</sup> - °K]/W)
	1.8	0.76	0.45	
<b>Roof layers details (Inside to outside)</b>				
Layers	Thickness (mm)	Density (kg/m <sup>3</sup> )	Specific Ht. (kJ/[kg - °K])	R-Value ([m <sup>2</sup> - °K]/W)
gypsum plaster	15.00	800	1.09	0.054
Stainless steel	180.00	8000	460	0.01
Air space	0	0	0	0.16026
Galvanized sheet	7.5	7850	470	0.00012
<b>Total U value 0.6776 W/m<sup>2</sup>.K</b>		<b>total R-value: 1.4756 m<sup>2</sup>.K/W</b>		
<b>Floor detail</b>				
Layers	Thickness (mm)	Density (kg/m <sup>3</sup> )	Specific Ht. (kJ/[kg - °K])	R-Value ([m <sup>2</sup> - °K]/W)
Granit stone tile	30.00	2700	790	0.007
Concrete	100.0	1400.0	913	0.188
<b>Total U value 13153.84 W/m<sup>2</sup>.K</b>		<b>total R-value: .000076 m<sup>2</sup>.K/W</b>		

The windows were designed based on their proportion to the façade, and a slider was assigned for each side of the facade (north, south, east, and west). For the northern and southern fronts, the range was set between 0.2 and 0.9. Because at intervals of zero, classes without windows appear, and in values of one, a glass wall. The east and west windows ranged from 0 to 0.9 because there was no necessity for east and west windows, and the design process was allowed to remove these windows. Window shades ranged from 10 to 90 centimeters. Shades are not set for the north windows. According to the sun path of Tabriz, the north windows are not exposed to direct sunlight.

For windows OKB, a conditional process was defined so that if the area of windows is more than or equal to 40% of the facade surface, its value is 90 cm, and if it is less than 40%, its value is equal to 1 meter and 10 cm.

In the end, shaders are assigned to the south façade at the top of the windows. Their range differs from 10 to 90 CM.

## **SIMULATION**

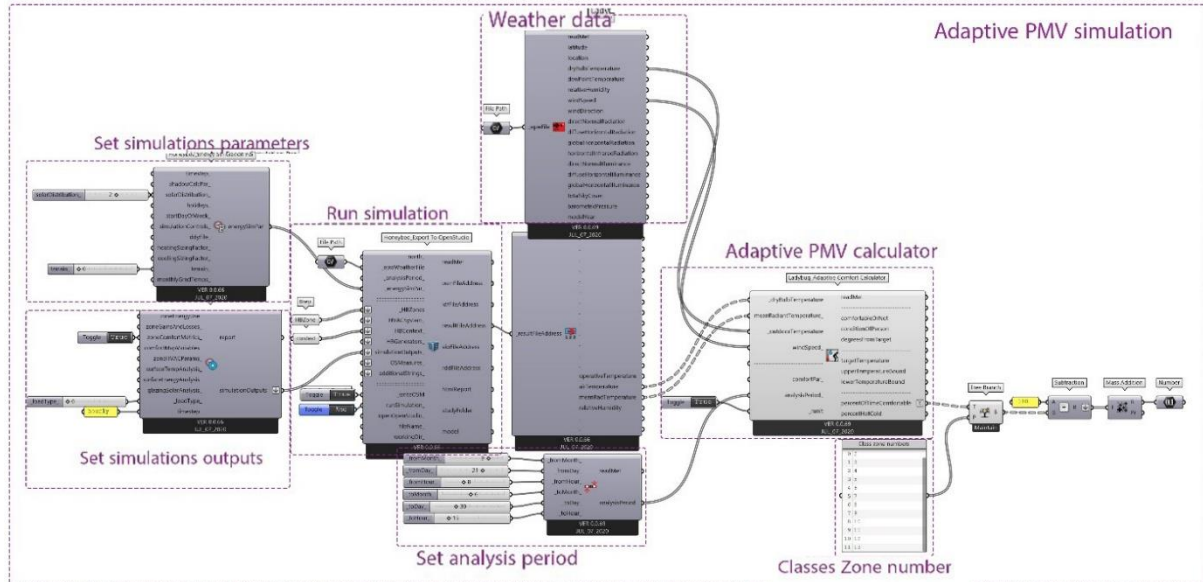
The school is located in Tabriz, one of the cities in Iran. Its weather is cold in winter and hot in summer. It could be said that it has an arid and cold climate. This study used the climatic data of Tabriz in its simulations. The weather file used in this study is for Tabriz Airport, with a latitude of 38-05N and a longitude of 046-17E, located at an elevation of 1367 m. The file is available for download from the Energy Plus website [29].

### **Thermal Comfort**

The adaptive PMV model is used in this article as a thermal comfort indicator. According to ASHRAE 55 [30], it is a model that regulates the internal temperature or acceptable temperature range with external climatological or metrological parameters and is estimated based on the climatic conditions outside the building. Most researchers have found that our feelings of comfort are influenced not only by human physiology and heat transfer mechanisms but also by social factors and psychological reactions to the environment [31]. The Open Studio engine in the Honeybee was used, and the adaptive thermal comfort factor was measured to simulate the amount of thermal comfort (Figure.7). Thermal comfort is estimated for each classroom, but because adjacent areas are vital for calculating thermal comfort in a school, all thermal zones of the school building were defined by the simulator engine to calculate thermal comfort. The Ladybug adaptive comfort calculator output is presented as a percentage of how much the space is within the comfort range for each defined zone. As a result, the values of 12 classes at the researched schools were extracted from the calculator's output. Because the optimization process is based on minimization, these numbers were calculated as 100-x to represent the percentage of hours when the space is thermally uncomfortable. Since the purpose of this article is to study the school in an integrated way, the thermal comfort of all 12 classes in the school model must be entered as a comprehensive value into the optimization process. Since the goal of this article is to investigate the school holistically, the thermal comfort of all 12 classes in the school model must be entered as a comprehensive value into the optimization process. As a consequence, the percentage of uncomfortable hours for each of the 12 classes was summed up, and the numerical result

was established as the thermal comfort index for the optimization algorithm. In other words, the quantity recognized by the optimization algorithm as thermal comfort and targeted to decrease as one of the objective functions is the sum of the percentage of hours of thermal discomfort in the school model's 12 classes. This number can vary from 0 to 1200.

Figure 7: Thermal comfort simulation workflow



## Visual Comfort

Daylight glare probability (DGP) is used as a visual comfort performance indicator. DGP is a short-term, local, single-domain index that assesses glare [32], introduced in 2005 by Wienold & Christoffersen [33], and approved in 2006 [34]. The critical thing about DGP is that although it was initially built to check for glare based on captured images, it can still be used to analyze glare in images from so-called rendering simulations. Therefore, according to Suk, Schiller [35] is the most appropriate criterion for analyzing glare issues. One limitation, however, is that it usually takes more time and effort than many other glare indicators that require simple analytical calculations. First, the designer must select one or more favorite positions, which are related to the primary occupant positions in space. RADIANCE image format renderings must be provided, and finally, a glare evaluation using Evalglare software, developed software that can detect light sources in the 180-degree scene of the fisheye, is done.

Wienold [36] also proposes a simplified version (DGP) in which the logarithmic term is ignored depending on local values (brightness and solid angle of the observed source from the point of view).

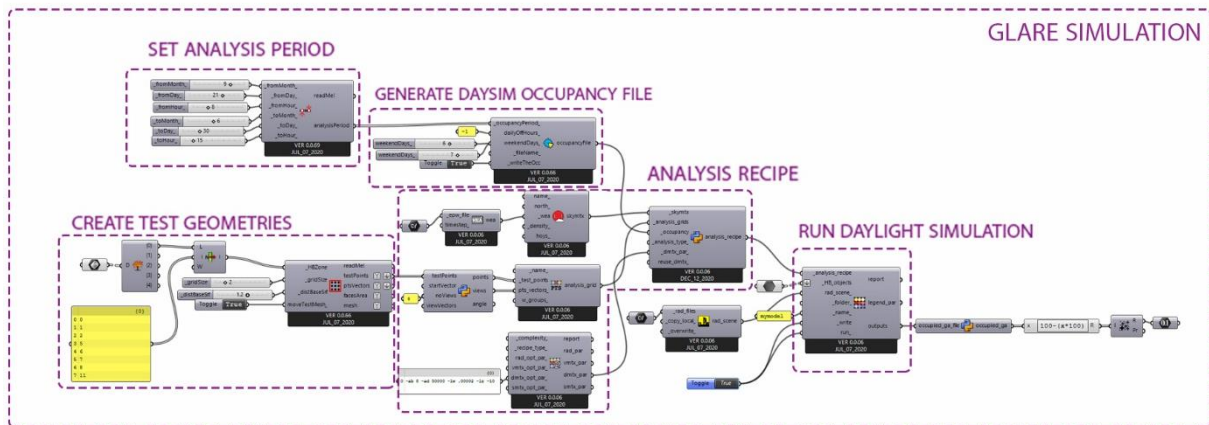
The disadvantage of DGP is that the analysis is time-consuming, as it is for different hours and days of the year. Nathaniel Jones [37] has introduced a method that can be used to calculate the annual glare in less time without the need for image rendering to solve this problem.

The imageless DGP achieves a rapid annual DGP simulation without removing contrast or hourly resolution factors. The basic idea is to replace the

luminosity and luminance conditions in DGP's equation with multi-phase method calculations. The imageless DGP is the method used in this article for glare analysis.

The Radiance engine in the Honeybee was used to calculate glare. The method proposed by Nathaniel L. Jones was used to achieving an annual imageless glare analysis (figure 8).

Figure 8: Visual comfort simulation workflow



Visual comfort, unlike thermal comfort, may be measured independently of nearby regions. Therefore, there is no need to involve all zones in the visual comfort process. To decrease simulation time, 8 classes with optically relevant positions were chosen among all the 12 classes for the investigation. All the southern front classes are defined in the plan in figure 6 with the titles of classes 1 and 2, and the classes that are exactly in the same position on the second floor. The East and West Front classes in the northern part of the school, which are introduced in figure 6 as classes 3 and 6, and the classes that are in the same position on the second floor, are a total of 8 classes. For each class, a network with a distance of 2 x 2 meters at the height of a sitting person was imagined, which included 60 points. These 60 points represent 60 people sitting in various spots across the classroom to examine the various orientations that these observers can have in the classroom; eight directions were chosen. To measure thermal comfort in different directions for the observer, he is turned at a 45-degree angle at a fixed point in the classroom. So, in this school, if 60 observers are considered, each of which is positioned in 8 distinct directions, 480 points are established to compute the visual comfort of the computing engine.

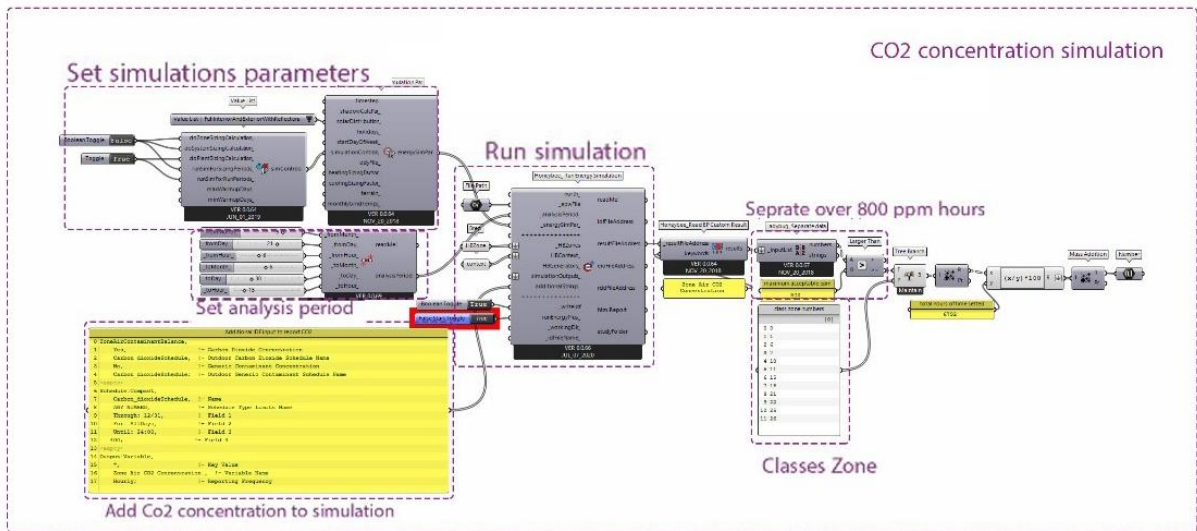
## Indoor Air Quality

The CO<sub>2</sub> concentration is generally used to express IAQ in terms of the ventilation required to reduce the concentration of indoor air pollutants [38]. Indoor CO<sub>2</sub> is a good indicator of indoor air quality [39], and relationships between CO<sub>2</sub> and indoor air quality have been well documented [40]. The standards for minimum rates of ventilation are specified in indoor quality standards such as ASHRAE [30], Standard 62, and EN15251 [41].

According to studies [42], CO2 concentrations over 1000 ppm could affect the occupant's health.

The Energy Plus engine was used to measure this factor in this model. Energy Plus is one of the most common and widely used energy simulation programs that can calculate the amount of CO2 production (based on occupancy) and predict its concentration based on the amount of production or reduction caused by external air intrusion (Figure 9).

Figure 9: CO2 concentration simulation workflow



## Optimization

Thermal comfort was calculated as the percentage of hours that the classrooms suffer from thermal dissatisfaction, and their sum was introduced as the second function of the optimization algorithm.

$$\text{Equation (2)} \quad F(x_1) = \sum(\text{Percentage of uncomfortable time spent in each class})$$

Because there are 12 classes in the model, the result of  $F(x_1)$  could be from 0 to 1200.

Visual comfort was introduced to the algorithm as the third function.

$$\text{Equation (3)} \quad F(x_2) = \sum(\text{percentage of hours with glare in points defined in each class})$$

Because there are 59 points in the analysis grid and every point is analyzed in 8 directions, the result of  $F(x_1)$  could be from 0 to 47200.

To optimize the IEQ, the concentration of carbon dioxide in the classrooms during the months when the schools are open and between 8 to 15 o'clock, which was above 800 ppm, was extracted, and the percentage was calculated for each class. The sum of these percentages is defined as the first function for minimization.

$$\text{Equation (4)} \quad F(x_3) = \sum(\text{number of hours in which CO2 concentration exceeds 800 ppm in each class})$$

Because there are 12 classes in the model, the result of  $F(x_3)$  could be from 0 to 1200.

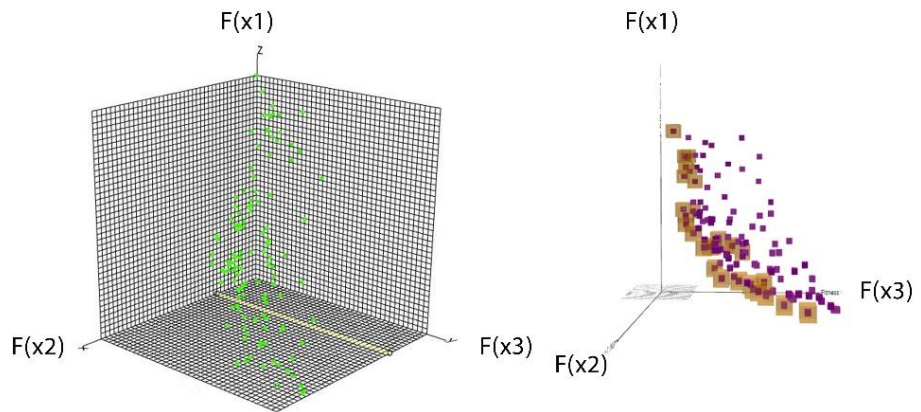
The Wallacei plugin is used in the optimization process. The platform performs its calculations as the primary evolutionary algorithm under the NSGA-2 algorithm.

Table 3. Optimization algorithm settings

Optimization algorithm settings	Value
Population	Generation size =30 Generation count =9
Crossover Probability (0.0 to 1.0)	0.8
Mutation Probability(0.0 to 1.0)	1/n (n is the number of variables in the problem, which in this case is 14)
Crossover and Mutation Distribution Index (0 to 100)	20

Wallacei runs for 72 hours on a computer equipped with an Intel(R) Core (TM) i7-2600K CPU running at 3.40 GHz and 16 GB of RAM. The process includes 270 glare, thermal comfort, and Co2 concentration simulations. It includes 9 generations with 30 individuals representing the Pareto front in figure 10. The three axes of the Pareto front represent thermal discomfort on the X-axis, visual discomfort on the Y-axis, and CO2 concentration of over 800 ppm on the Z-axis. Points near the center of the graph are closer to the algorithm's targets. The minimum concentration of carbon dioxide and thermal and visual discomfort is expected in this paper.

Figure 10: Pareto front



## RESULTS

The plans and masses created in the last generation are shown in figures 11 and 12 as a sample of outcomes.

Figure 11: Masses of schools created in the last generation

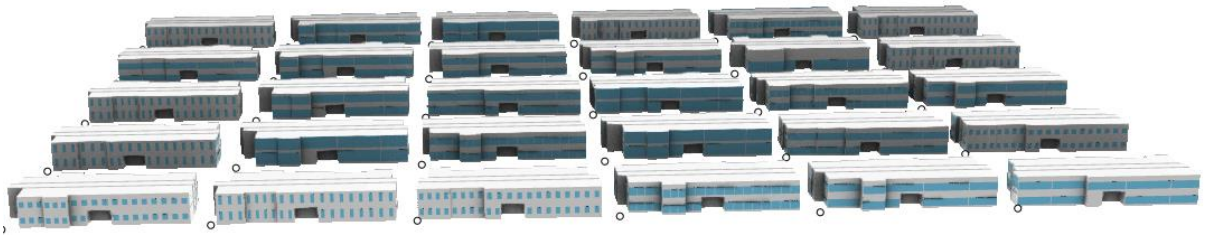
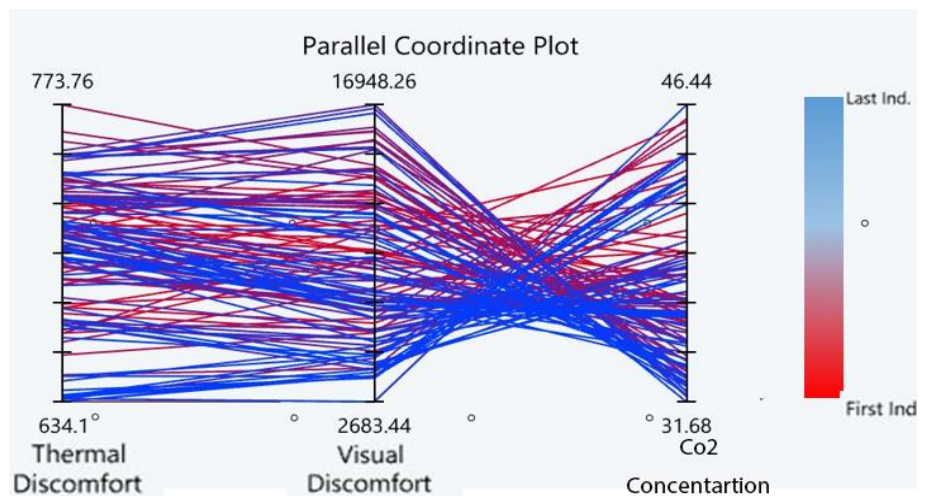


Figure 12: Plans of schools created in the last generation



The Parallel Coordinate Plot (PCP) diagram analyzes all the solutions in the population by comparing the values of the functions for each solution in all the objective functions. The aim is to extract the simulated emerging behaviors and to understand better how the optimization process works (Figure.13).

Figure 13: The Parallel Coordinate Plot (PCP) diagram



The fitness values diagram analyzes the values of functions for each objective function independently in the whole population. The goal is to visualize how solutions work concerning each other in each generation and among the population.

Solutions are displayed in each generation from left to right (the first point on the y-axis is the first solution in a generation, and the last point on the y-axis is the final solution in the same generation). Each generation is associated with a multi-line, and the generations are colored from the first (red) to the last (blue).

Since the target of optimization is to minimize the fitness value, it is expected that the blue colors, which represent the last generation, will be at the bottom of the charts and the red colors will be at the top. However, as seen in figures 14–16, the colors blue and red are scattered across the whole surface of the graph, indicating that the fitness values of the last generations have not decreased across the whole population. This occurrence could indicate that the algorithm seeks to minimize the three functions defined for it and that the minimum of one function is likely to be the maximum of the other, implying that the algorithm was unable to uniformly reduce the fitness values of all individuals in the last generation.

Figure 14: Fitness values diagram of thermal discomfort

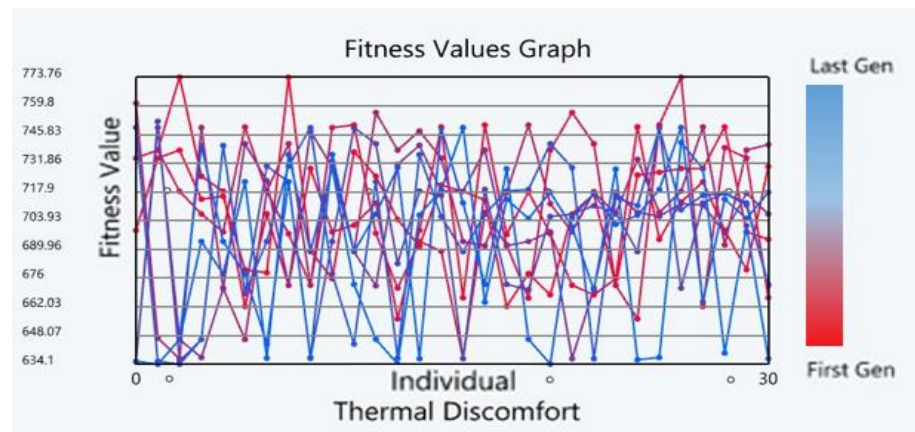


Figure 15: Fitness values diagram of visual discomfort

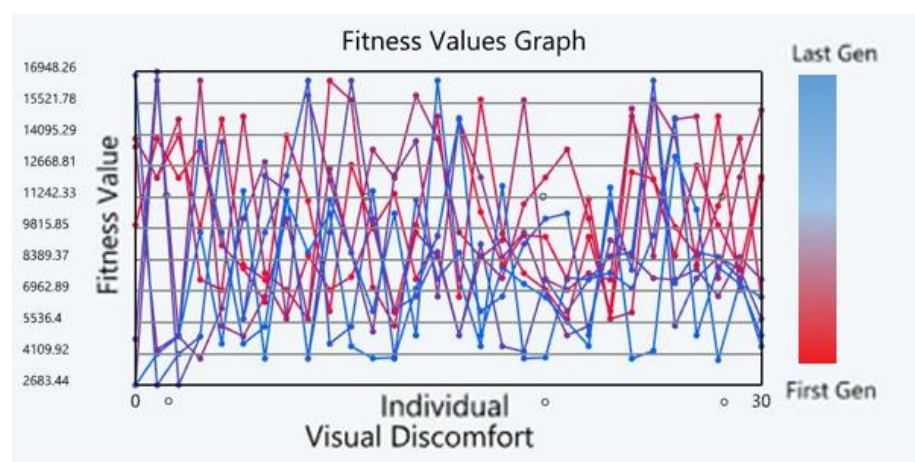
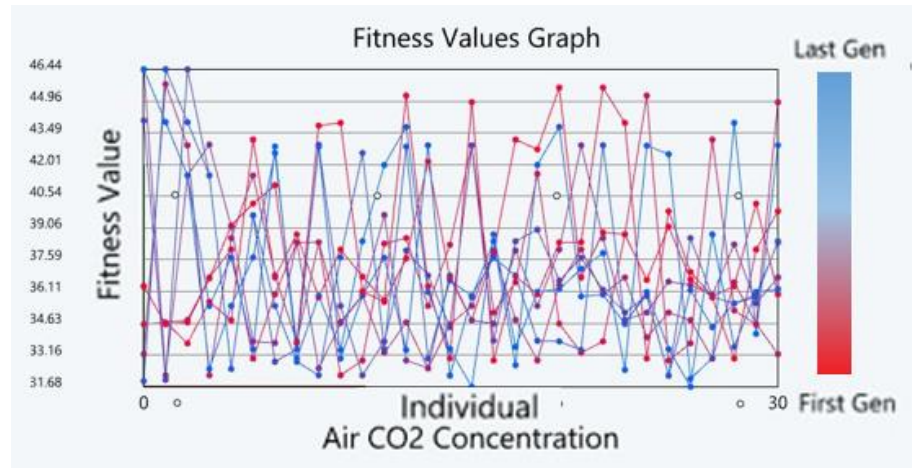


Figure 16: Fitness values diagram of co2 concentration



The range of thermal comfort change, as indicated in figures 13 and 14, is from 773.76 to 634.1, whereas the explanations in the preceding sections imply that this ratio can range from 0 to 1200. The difference is 139.66. Since these values are the sum of the percentages of discomfort hours from 12 classes, dividing them by 12 can obtain the average of the classes' thermal discomfort. As a result, the percentage change in the classes' average thermal discomfort among studied models is 11.63 percent. The best record produced in the procedure outperformed the worst by 11.63 percent.

In the same way, the minimum record registered in the process of CO<sub>2</sub> concentration optimization performed 0.199% better than the maximum one. It means the design variables that are studied in this article do not have much influence on the building's CO<sub>2</sub> concentration or the experiment condition is not a proper way to analyze this factor of IEQ.

In figures 13 and 15, the range of visual comfort change is from 16948.26 to 2663.44. The difference is 14,284.82, which is the sum of the percentage of hours of visual discomfort at the 480 points entered in the visual comfort analysis process, which was explained in the previous sections. By dividing by 480, we achieve the average change of one point, which will be equal to 29.76%.

So, the minimum record registered in the process is performed 29.76% better than the maximum one.

The mean value trendline diagram shows the average of the fitness functions for each objective function independently, and for each generation in the whole simulation from beginning to end. The goal is to identify specific trends in the mean value of each generation function among the population.

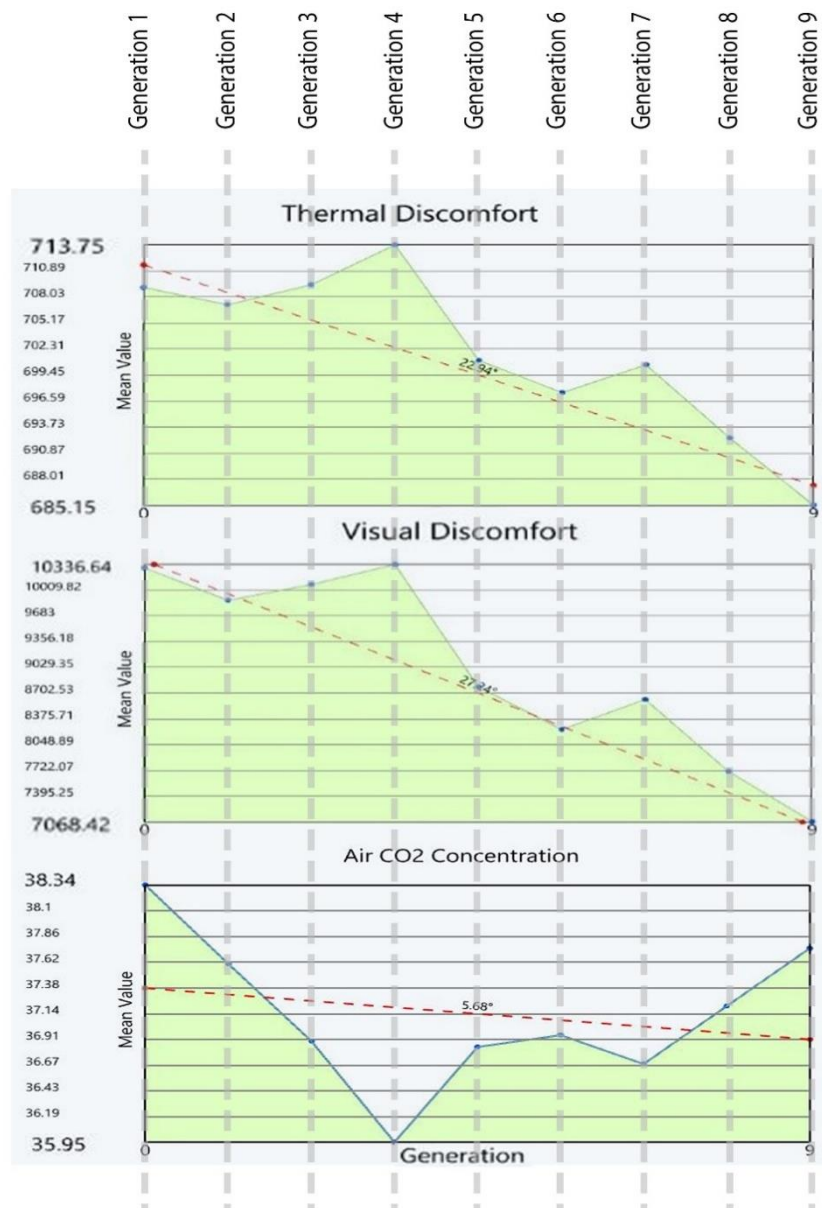
This diagram shows the average value of each function as a point from the left (first generation) to the right (last generation).

According to this diagram, the functions of thermal comfort and visual comfort are directly related to each other and, at the same time, are inversely related to the concentration of CO<sub>2</sub> so that the peak points in the graphs of thermal

and visual comfort are at the bottom of the carbon dioxide concentration graph.

As seen in figure 17, visual and thermal comfort behave in tandem, whereas carbon dioxide concentrations behave in the opposite direction. For example, in the fourth generation, indexes of thermal and visual discomfort have climbed to the top of their charts, whilst carbon dioxide concentration meets the bottom of its chart. It refers to the relationship of each factor with the glazing ratio of the building.

Figure17: The mean value trendline diagram of thermal, and visual discomfort, and Co2 concentration



The standard deviation represents the distribution of a set of values from the mean. A low standard deviation indicates that most values are accumulated in the average range (more minor variation in the population). In contrast, a high standard deviation indicates that the values are more comprehensive than the average (more variation in the population). The purpose of the diagram is to present and analyze the levels of diversity and convergence for each generation in the population, as well as whether the generations are becoming fitter during the simulation. The flat curve means an increase in variability, while the narrow curve shows an increase in convergence in the population. Moving the curves to the left indicates better average performance.

According to figure 18, the dispersion of genes in generations is increasing (since the blue curves that belong to the later generations have lower and less abrupt peaks). This may be because among the factors studied, for example, those whose increase reduces thermal and visual discomfort, at the same time increasing the concentration of carbon dioxide. However, moving the center of the curves to the left indicates a decrease in the mean during the optimization process.

The changes in the glass ratio of different facades in suitable samples of each fitness value show that the WWR ratio is the most influential variable among the design variables.

The low WWR for the south façade results best in the thermal and visual comfort models, and inversely, the higher amount of it produces the best result for CO<sub>2</sub> concentration.

Generally, the performance of the best cases introduced by the algorithm is more appropriate than the design prototype. However, the results show that the difference in models in terms of carbon dioxide concentration is negligible. According to table 5, the base model's performance is near the best result introduced by the algorithm for thermal comfort.

Regarding visual comfort, the result of the algorithm shows 4% better performance than the base model.

The comparison is shown in table 6 to visualize the improvement of IEQ performance of each field's best result with the base model. The CO<sub>2</sub> concentration detailed shown in the table does not exceed over 1000 ppm in an hour, so the overall best answer to IEQ performance is chosen from the result models, which have the best daylighting and thermal performance.

Figure18: standard deviation graph of thermal, and visual discomfort, and Co2 concentration

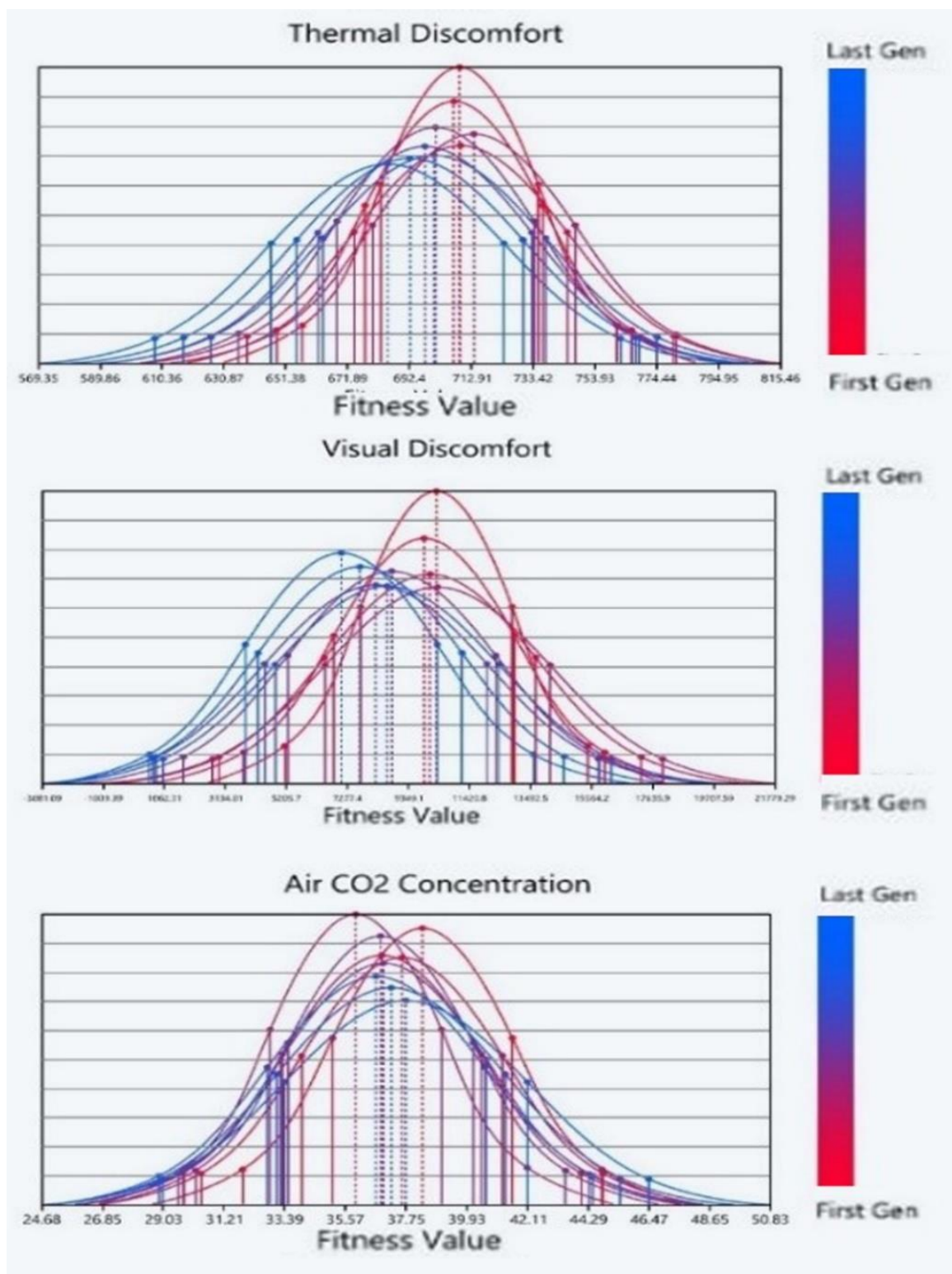


Table 4: The two best models of each fitness function.

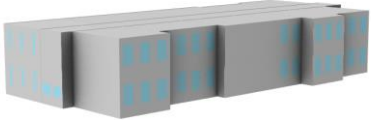
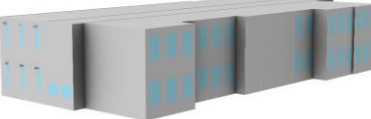
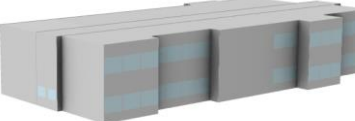
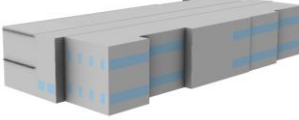
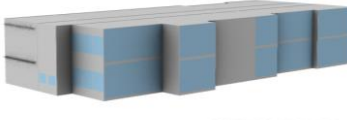
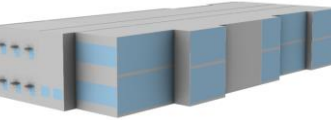
Position in the population	Northeast view	Southwest view
Generation No. 8 Individual No. 1		
Generation No. 8 Individual No. 12		
Generation No. 8 Individual No. 0		
Generation No.8 Individual No.27		
generation No.8 Individual NO.15		
Generation NO.6 Individual NO.0		

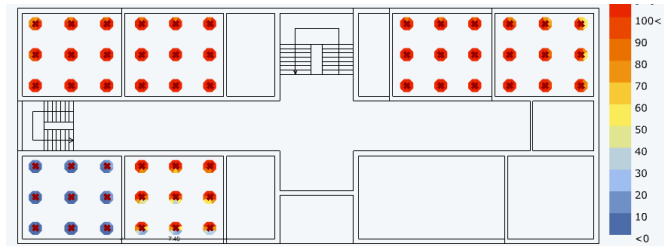
Table 5: the variable of base and best models  $f(x)1=\Sigma(\text{thermal discomfort})$ ,  $f(x)2=\Sigma(\text{visual discomfort})$ ,  $f(x)3=\Sigma(\text{IQO inappropriate})$

	V.1	V.2	V.3	V.4	V.5	V.6	V.7	V.8	V.9	V.10	V.11	V.12	V.13	V.14	f(x)1	f(x)2	f(x)3
Base model	7	7	7	7	7	7	1.2	1.2	0	0.3	0	0.3	0	0	655.32	4687.6	43.80
Thermal best solutions																	
Gen8 ind1	6.35	7.07	5.89	7.64	5.17	6.22	1.9	2	0.4	0.2	0.1	0	0.3	0.29	634.09	4105.38	43.97
Gen8 ind12	6.36	7.07	5.88	7.64	5.17	5.05	1.9	2	0.4	0.2	0.1	0	0.3	0.29	634.23	3941.93	43.75
Visual best solution																	
Gen8 ind0	5.75	5.33	6.41	7.8	5.22	7.91	1.5	1.3	0.1	0.2	0	0.4	0	0.29	635.55	2683.44	46.43
Gen8 ind27	7.47	7.07	5.87	7.48	6.64	7.88	2	1.3	0.4	0.5	0	0.3	0.3	0.35	639.75	3827.58	42.93
Co2 best solutions																	
Gen8 ind15	6.62	7.66	7.68	5.19	7.96	7.1	1.9	1.1	0.9	0.8	0.5	0.9	0.7	0.45	749.24	14843.07	31.68
Gen6 ind0	6.7	7.76	7.67	5.63	7.96	6.97	1.8	1	0.9	0.8	0.5	0.9	0.8	0.73	749.29	16779.02	31.94

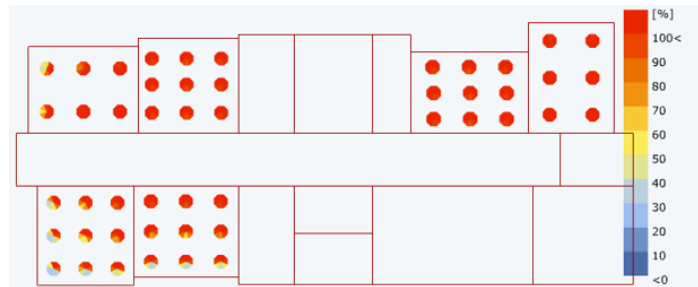
Table 6: Comparison of the best sample performance with the base model

Glare Autonomy(the fraction of occupied hours in which the view is free of glare) comparison between the base model and Rank 1 visual comfort solution

Base model's glare autonomy (the fraction of occupied hours in which the view is free of glare)

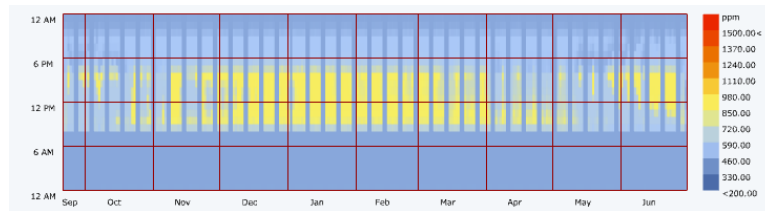


Rank1 visual comfort's glare autonomy (the fraction of occupied hours in which the view is free of glare)

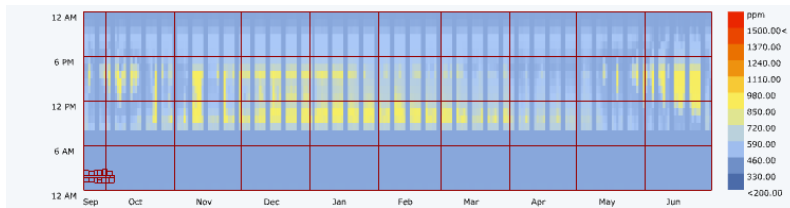


Zone Class NO.1 CO2 Concentration (ppm) hourly From 21 September till 30 June

Base model

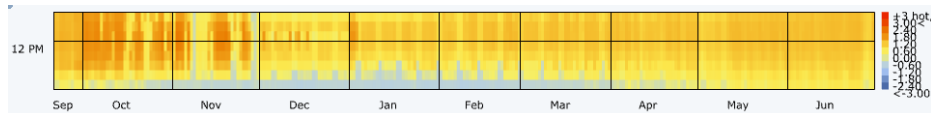


Rank1 CO2 Concentration

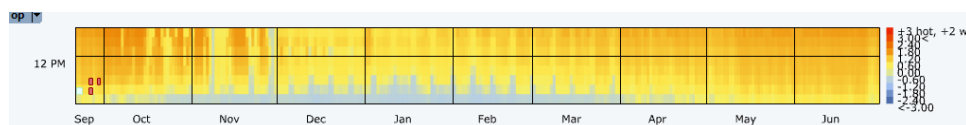


Zone Class NO.1 PMV hourly From 21 September till 30 June

Base model



Rank1 Thermal comfort



## CONCLUSION

Based on the importance of IEQ in the efficiency and productivity of school buildings, it is necessary to find a comprehensive method for its assessment in the early stages of building design.

It is also significant to define verifiable standards. Among the research projects about interior environmental quality (IEQ) in schools, most of them refer to one or two aspects of it. This paper focused on representing the details of parametric-based optimization using genetic algorithms in Grasshopper to provide a platform for integrated IEQ analysis. A school model was introduced to develop thermal and visual comfort and CO<sub>2</sub> concentration performance. Many parameters were affecting IEQ, such as WWR, class dimensions, and shading devices. The optimization process consists of 9 generations. The solutions have formed different diagrams and charts, which were very helpful in showing what happened during the process. The algorithm finds the best answer for each fitness function. While illustrating the optimum solution, it is found that there is a direct relationship between visual and thermal comfort and an indirect relationship between them and CO<sub>2</sub> concentration.

Optimization algorithms have the appropriate capacity to be used in architectural decision-making. A remarkable point is the ability of designers to define the design problem in a parametric language. It should also be noted that the more appropriate and limited the definition of the design problem, the clearer the answers are received. However, the role of the architect cannot be eliminated because what these algorithms provide are answers that are close to the goal that is set. The judgment of its accuracy depends on the opinion of the designer, but the use of the power of this algorithm is a tool that helps architects in design, presenting different proposals and categorizing them at the right time.

## REFERENCES

1. Fisk, W.J., *Review of health and productivity gains from better IEQ*. 2000.
2. Fisk, W.J., *How IEQ affects health, productivity*. ASHRAE journal, 2002. 44(LBNL-51381).
3. Fisk, W.J., D. Black, and G. Brunner, *Benefits and costs of improved IEQ in US offices*. *Indoor Air*, 2011. 21(5): p. 357-367. <https://doi.org/10.1111/j.1600-0668.2011.00719.x>
4. Diaz, M., M.B. Piderit, and S. Attia. *Parameters and indicators used in Indoor Environmental Quality (IEQ) studies: a review*. in *Journal of Physics: Conference Series*. 2021. IOP Publishing. <https://doi.org/10.1088/1742-6596/2042/1/012132>
5. Wei, W., et al., *Review of parameters used to assess the quality of the indoor environment in Green Building certification schemes for offices and hotels*. *Energy and Buildings*, 2020. 209: p. 109683. <https://doi.org/10.1016/j.enbuild.2019.109683>
6. Asadi, I., N. Mahyuddin, and P. Shafigh, *A review on indoor environmental quality (IEQ) and energy consumption in building based on occupant behavior*. *Facilities*, 2017. <https://doi.org/10.1108/F-06-2016-0062>
7. Pereira, L.D., F.B. Lamas, and M.G. da Silva, *Improving energy use in schools: from IEQ towards energy-efficient planning—method and in-field application to two case studies*. *Energy Efficiency*, 2019. 12(5): p. 1253-1277. <https://doi.org/10.1007/s12053-018-9742-5>
8. Catalina, T. and V. Lordache, *IEQ assessment on schools in the design stage*. *Building and Environment*, 2012. 49: p. 129-140. <https://doi.org/10.1016/j.buildenv.2011.09.014>
9. Karapetsis, A. and E. Alexandri. *Indoor Environmental Quality and its Impacts on Health—Case Study: School Buildings*. in *Proceedings of the EinB2016—5th*

International Conference "ENERGY in BUILDINGS. 2016.

<https://doi.org/10.1155/2021/8851685>

10. Kabele, K., Z. Veverková, and M. Urban. *Methodology for assessing the indoor environmental quality in low energy buildings in the Czechia*. in *IOP Conference Series: Materials Science and Engineering*. 2019. IOP Publishing. <http://dx.doi.org/10.1088/1757-899X/609/4/042103>

11. Wei, L., et al., *Effects of building form on energy use for buildings in cold climate regions*. *Procedia Engineering*, 2016. **146**: p. 182-189.

<https://doi.org/10.1016/j.proeng.2016.06.370>

12. Bahaj, A.S., P.A. James, and M.F. Jentsch, *Potential of emerging glazing technologies for highly glazed buildings in hot arid climates*. *Energy and Buildings*, 2008. **40**(5): p. 720-731. <http://dx.doi.org/10.1016/j.enbuild.2007.05.006>

13. Hollberg, A. and J. Ruth, *LCA in architectural design—a parametric approach*. *The International Journal of Life Cycle Assessment*, 2016. **21**(7): p. <http://dx.doi.org/943-960>. [10.1007/s11367-016-1065-1](https://doi.org/10.1007/s11367-016-1065-1)

14. Holzer, D., R. Hough, and M. Burry, *Parametric design and structural optimisation for early design exploration*. *International Journal of Architectural Computing*, 2007. **5**(4): p. 625-643.

<https://doi.org/10.1260/2F147807707783600780>

15. Machairas, V., A. Tsangrassoulis, and K. Axarli, *Algorithms for optimization of building design: A review*. *Renewable and sustainable energy reviews*, 2014. **31**: p. 101-112. <https://doi.org/10.1016/j.rser.2013.11.036>

16. Holland, J., *Adaptation in natural and artificial systems*, univ. of mich. press. Ann Arbor, 1975.

17. Frazer, J., *An evolutionary architecture*. 1995.

18. Wang, W., R. Zmeureanu, and H. Rivard, *Applying multi-objective genetic algorithms in green building design optimization*. *Building and environment*, 2005. **40**(11): p. 1512-1525. <https://doi.org/10.1016/j.buildenv.2004.11.017>

19. Ooka, R. and K. Komamura, *Optimal design method for building energy systems using genetic algorithms*. *Building and Environment*, 2009. **44**(7): p. 1538-1544. <https://doi.org/10.1016/j.buildenv.2008.07.006>

20. Toutou, A., M. Fikry, and W. Mohamed, *The parametric based optimization framework daylighting and energy performance in residential buildings in hot arid zone*. *Alexandria engineering journal*, 2018. **57**(4): p. 3595-3608.

<https://doi.org/10.1016/j.aej.2018.04.006>

21. Buratti, C., et al., *Unsteady simulation of energy performance and thermal comfort in non-residential buildings*. *Building and Environment*, 2013. **59**: p. 482-491. <https://doi.org/10.1016/j.buildenv.2012.09.015>

22. Mazzeo, D. and K.J. Kontoleon, *The role of inclination and orientation of different building roof typologies on indoor and outdoor environment thermal comfort in Italy and Greece*. *Sustainable Cities and Society*, 2020. **60**: p. 102111. <https://doi.org/10.1016/j.scs.2020.102111>

23. Latha, P., Y. Darshana, and V. Venugopal, *Role of building material in thermal comfort in tropical climates—A review*. *Journal of Building Engineering*, 2015. **3**: p. 104-113. <https://doi.org/10.1016/j.jobe.2015.06.003>

24. Singh, M., S. Garg, and R. Jha, *Different glazing systems and their impact on human thermal comfort—Indian scenario*. *Building and Environment*, 2008. **43**(10): p. 1596-1602. <https://doi.org/10.1016/j.buildenv.2007.10.004>

25. Lyons, P.R., D. Arasteh, and C. Huizenga, *Window performance for human thermal comfort*. *Transactions-American Society of Heating Refrigerating and Air Conditioning Engineers*, 2000. **106**(1): p. 594-604.

26. Middel, A., et al., *Impact of shade on outdoor thermal comfort—a seasonal field study in Tempe, Arizona*. *International journal of biometeorology*, 2016. **60**(12): p. 1849-1861. <https://doi.org/10.1007/s00484-016-1172-5>

27. Lee, E.S. and A. Tavit, *Energy and visual comfort performance of electrochromic windows with overhangs*. *Building and Environment*, 2007. **42**(6): p. 2439-2449. <https://doi.org/10.1016/j.buildenv.2006.04.016>

28. Tzempelikos, A. and Y.-C. Chan, *Estimating detailed optical properties of window shades from basic available data and modeling implications on daylighting and visual comfort*. *Energy and Buildings*, 2016. **126**: p. 396-407.

<https://doi.org/10.1016/j.enbuild.2016.05.038>

29. *energy plus weather data*. 2021: [https://energyplus.net/weather-location/asia\\_wmo\\_region\\_2/IRN/IRN\\_Tabriz.407060\\_ITMY](https://energyplus.net/weather-location/asia_wmo_region_2/IRN/IRN_Tabriz.407060_ITMY).

30. Handbook-Fundamentals, A. and S. Edition, *Atlanta: American Society of Heating, Refrigerating and Air-Conditioning Engineers*. Inc.(see page 14.14 for

summary description of RP-1171 work on uncertainty in design temperatures), 2009.

31. Choudhury, A.R., P. Majumdar, and C. Datta, *Factors affecting comfort: human physiology and the role of clothing*, in *Improving comfort in clothing*. 2011, Elsevier. p. 3-60. <https://doi.org/10.1533/9780857090645.1.3>
32. Chaloeitoy, K., M. Ichinose, and S.-C. Chien, *Determination of the Simplified Daylight Glare Probability (DGPs) Criteria for Daylit Office Spaces in Thailand*. *Buildings*, 2020. **10**(10): p. 180. <https://doi.org/10.3390/buildings10100180>
33. Wienold, J. and J. Christoffersen, *Towards a new daylight glare rating*. Lux Europa, Berlin, 2005: p. 157-161.
34. Wienold, J. and J. Christoffersen, *Evaluation methods and development of a new glare prediction model for daylight environments with the use of CCD cameras*. *Energy and buildings*, 2006. **38**(7): p. 743-757. <https://doi.org/10.1016/j.enbuild.2006.03.017>
35. Suk, J.Y., M. Schiler, and K. Kensek, *Development of new daylight glare analysis methodology using absolute glare factor and relative glare factor*. *Energy and Buildings*, 2013. **64**: p. 113-122. <https://doi.org/10.1016/j.enbuild.2013.04.020>
36. Wienold, J. *Dynamic simulation of blind control strategies for visual comfort and energy balance analysis*. in *Building Simulation*. 2007. IBPSA Beijing.
37. Jones, N.L., *The Imageless Method for Spatial and Annual Glare Analysis*. 2019: <https://github.com/nljones/Accelerad/wiki/The-Imageless-Method-for-Spatial-and-Annual-Glare-Analysis>.
38. Wargocki, P., et al., *The effects of outdoor air supply rate in an office on perceived air quality, sick building syndrome (SBS) symptoms and productivity*. *Indoor air*, 2000. **10**(4): p. 222-236. <https://doi.org/10.1034/j.1600-0668.2000.010004222.x>
39. Kapalo, P., S. Vilcekova, and O. Voznyak, *Using experimental measurements of the concentrations of carbon dioxide for determining the intensity of ventilation in the rooms*. *Chemical Engineering Transactions*, 2014. **39**: p. 1789-1794. <https://doi.org/10.3303/CET1439299>
40. Persily, A.K., *Evaluating building IAQ and ventilation with indoor carbon dioxide*. 1997, American Society of Heating, Refrigerating and Air-Conditioning Engineers.
41. Comite'Europe'en de Normalisation, C., *Indoor environmental input parameters for design and assessment of energy performance of buildings addressing indoor air quality, thermal environment, lighting and acoustics*. EN 15251, 2007.
42. Cetin, M., *A Change in the Amount of CO<sub>2</sub> at the Center of the Examination Halls: Case Study of Turkey*. *Studies on Ethno-Medicine*, 2016. **10**(2): p. 146-155. <https://doi.org/10.1080/09735070.2016.11905483>

**Submetido: 13/12/2021**

**Aceito: 01/07/2022**